THE JOURNAL OF BIOLOGICAL CHEMISTRY VOL. 287, NO. 31, pp. 26268–26277, July 27, 2012

Trypanosoma brucei 20 S Editosomes Have One RNA Substrate-binding Site and Execute RNA Unwinding Activity*[S]

Received for publication, March 23, 2012, and in revised form, May 10, 2012 Published, JBC Papers in Press, June 1, 2012, DOI 10.1074/jbc.M112.365916

Cordula Böhm[1], **Venkata Subbaraju Katari, Michael Brecht, and H. Ulrich Göringer**[2]

From the Department of Molecular Genetics, Darmstadt University of Technology, 64287 Darmstadt, Germany

Background: Mitochondrial transcripts in African trypanosomes undergo U insertion/deletion-type RNA editing that is catalyzed by a protein complex known as the editosome.
Results: Editosomes have a single RNA substrate-binding site and catalyze RNA unwinding.
Conclusion: Both U insertion and U deletion are executed within a single, multifunctional reaction center.
Significance: RNA binding is followed by RNA unwinding, which represents a novel activity of the editing machinery.

Editing of mitochondrial pre-mRNAs in African trypanosomes generates full-length transcripts by the site-specific insertion and deletion of uridylate nucleotides. The reaction is catalyzed by a 0.8 MDa multienzyme complex, the editosome. Although the binding of substrate pre-edited mRNAs and cognate guide RNAs (gRNAs) represents the first step in the reaction cycle, the biochemical and biophysical details of the editosome/RNA interaction are not understood. Here we show that editosomes bind full-length substrate mRNAs with nanomolar affinity in a nonselective fashion. The complexes do not discriminate–neither kinetically nor thermodynamically–between different mitochondrial pre-mRNAs or between edited and unedited versions of the same transcript. They also bind gRNAs and gRNA/pre-mRNA hybrid RNAs with similar affinities and association rate constants. Gold labeling of editosome-bound RNA in combination with transmission electron microscopy identified a single RNA-binding site per editosome. However, atomic force microscopy of individual pre-mRNA-editosome complexes revealed that multiple editosomes can interact with one pre-mRNA. Lastly, we demonstrate a so far unknown activity of the editing machinery: editosome-bound RNA becomes unfolded by a chaperone-type RNA unwinding activity.

Mitochondrial gene expression in kinetoplastid protozoa such as African trypanosomes requires RNA editing. The reaction converts cryptic pre-mRNAs into mature transcripts and is characterized by the insertion and deletion of exclusively U[3] nucleotides (for recent reviews see Refs. 1 and 2). The process involves a specific class of small, noncoding RNAs, known as guide RNAs (gRNAs), which represent transacting genetic elements that function as templates in the process (3). The basic reaction steps of the editing reaction cycle involve ribonuclease (4–9), uridylyl transferase (10, 11), RNA ligase (12–14), and perhaps nucleotidyl phosphatase activities (15). In addition, accessory factors such as matchmaking-type RNA/RNA annealing factors (16–22) and RNA helicases (23, 24) have been shown to contribute. Protein candidates for every step of the basic reaction cycle have been identified, thereby confirming the general features of the enzyme-driven multistep pathway (3, 25). Importantly, all key editing enzymes are assembled in a single, high molecular mass mitochondrial complex, which has been termed the editosome (reviewed in Refs. 2 and 26). Editosomes provide a reaction platform for the individual steps of the processing reaction and have been isolated from steady state mitochondrial detergent extracts of African trypanosomes and *Leishmania tarentolae* (27, 28). Trypanosome editosomes have an apparent hydrodynamic size in the range of 20 S and have been visualized by cryoelectronmicroscopy at a resolution of approximately 2 nm. They are composed of two globular subdomains of roughly equal size that are connected by a small interface region. Editosomes have a calculated molecular mass of 0.8 MDa (27) and depending on the enrichment protocol consist of 13–20 polypeptides (for a recent review see Ref. 1). All of the proteins are nuclear encoded and the complex is free of RNA. Because the number of complex-assembled polypeptides exceeds the number of required enzyme activities, it has been suggested that some components have only a structural function (29). However, it cannot be excluded that editosomes harbor additional, so far unidentified enzymatic activities. 20 S editosomes have the ability to bind short, synthetic substrate RNAs and catalyze both U insertion and U deletion editing in a gRNA-dependent fashion (7, 30). Although the situation seems to differ between *Leishmania* and trypanosomes (27, 28), steady state isolates of *Trypanosoma brucei* editosomes contain editing complexes that are loaded with endogenous pre-mRNA/gRNA substrate RNAs. Because of the different sizes of the various pre-mRNAs, these complexes form a heterogeneous

* This work was supported by German Research Council Grant DFG-SFB902 and an International Research Scholar Grant of the Howard Hughes Medical Institute (to H. U. G.).
[S] This article contains supplemental Figs. S1–S4.
[1] Present address: Dept. of Pathology, University of Cambridge, Tennis Court Rd., Cambridge CB2 1QP, UK.
[2] To whom correspondence should be addressed: Dept. of Molecular Genetics, Darmstadt University of Technology, Schnittspahnstrasse 10, 64287 Darmstadt, Germany. Tel.: 49-6151-162855; Fax: 49-6151-165640; E-mail: goringer@hrzpub.tu-darmstadt.de.
[3] The abbreviations used are: U, uridylate; gRNA, guide RNA; AFM, atomic force microscopy; TAP, tandem affinity purification; EB, editing buffer; UE, unedited; FE, fully edited; COI, cytochromoxidase subunit I; bio, 5′-biotinylated; Cyb, apocytochrome *b*; A6, ATPase subunit 6; OB, oligonucleotide/oligosaccharide binding.

ensemble of particles with hydrodynamic values varying between 35 and 40 S (27). 35–40 S editosomes have a calculated molecular mass of up to 1.45 MDa (27) and consist of a slightly convex platform element that extends on both ends into globular head-like and foot-like protuberances. A three-dimensional alignment of the 20 S and 35–40 S complexes in conjunction with biochemical data identified that the 20 S complex represents a major part of the 35–40 S complex (27) and as a consequence supports a scenario in which substrate RNA binding and release are central determinants in the interconversion of the two complexes. Unfortunately, the molecular details of the editosome/RNA interaction are only marginally understood. Neither the number of RNA-binding sites per editosome, nor kinetic, thermodynamic, and/or selectivity and specificity issues have been addressed systematically. The situation is further complicated by the fact that compositionally different editosomes seem to exist in transgenic trypanosomes (31, 32) and that the complexes can associate with multiple RNA ligands: pre-edited, partially edited, and fully edited mRNAs as well as gRNAs and cognate gRNA/pre-mRNA pairs.

Here we present an analysis of the RNA binding characteristics of native *T. brucei* 20 S editosomes. We show high affinity RNA binding without discrimination between mRNA, gRNA, and mRNA/gRNA hybrid molecules and without discrimination between different mitochondrial transcripts or edited and unedited versions of the same transcript. We further demonstrate that 20 S editosomes have a single RNA-binding site, whereas multiple editosomes can interact with one RNA molecule. Finally, we demonstrate that RNA binding to 20 S editosomes is followed by an RNA unfolding reaction, which is catalyzed by a chaperone-type RNA unwinding activity of the editosome.

EXPERIMENTAL PROCEDURES

Preparation of Editosomes—20 S editosomes were isolated from mitochondrial vesicle preparations of procyclic stage *T. brucei* cells. The following strains were used: Lister 427 (33) and the transgenic cell line 29-13-TbMP42/TAP (27). Parasite cells were harvested at late log phase and disrupted by N_2 cavitation at isotonic conditions (34). Mitochondrial vesicles were isolated by differential centrifugation and used to prepare mitochondrial detergent extracts by incubation with 0.6% (v/v) Nonidet-P40 in editing buffer (EB): 20 mM HEPES/KOH, pH 7.5, 30 mM KCl, 10 mM $Mg(OAc)_2$, 0.5 mM DTT. 20 S editosomes were enriched by isokinetic ultracentrifugation in linear 10–35% (v/v) glycerol gradients (35). TAP-tagged 20 S editosomes were isolated from spin-cleared mitochondrial detergent extracts by consecutive IgG and calmodulin affinity chromatography followed by isokinetic ultracentrifugation in linear 10–35% (v/v) glycerol gradients. All editosome preparations were tested for their gRNA-dependent U insertion/U deletion *in vitro* RNA editing activity (7, 30). The protein composition of TbMP42/TAP editosomes has been described by Golas *et al.* (27).

RNA Oligonucleotide Synthesis and Biotinylation—RNA oligonucleotides were synthesized by solid phase phosphoramidite chemistry using 2′-*O*-triisopropylsilyloxymethyl-protected monomers. The U insertion substrate RNAs were 5′-mRNA fragment: GGAAGUAGAGAGUAGG, 3′-mRNA fragment: AUUGGAGUUAUAG-NH_2, and gRNA: CUAUAACCCGAUAAACCUACGUCUCAUACUUCC. The U deletion substrate RNAs were 5′-mRNA fragment: GGAAAGGGAAAGUUGUGAU-UUU, 3′-mRNA fragment: GCGAGUUAUAGAAUA-NH_2, and gRNA: GGUUCUAUAACUCGCUCACAACUUUCCCUUUCC. 5′-biotinylated oligoribonucleotides were synthesized using 2-aminoethoxy-ethoxyethanol-linked biotinylated phosphoramidites. Synthetic pre-mRNA/gRNA hybrid molecules were generated in EB by incubating equimolar concentrations of both RNAs at 65 °C for 5 min and cooling to room temperature at a rate of 1 °C/min.

RNA Transcription—Unedited (UE) and fully edited (FE) A6 (344 nucleotides/762 nucleotides), UE and FE apocytochrome *b* (Cyb) (1080 nucleotides/1113 nucleotides), and never edited cytochromoxidase subunit I (COI) (1647 nucleotides) transcripts were PCR-amplified from *T. brucei* Lister 427 cDNA preparations. PCR products were cloned into pBS SK^- (Stratagene) and sequenced. RNAs were synthesized by run-off transcription from linear DNA plasmid templates using T7 RNA polymerase following standard procedures. Guide RNA gA6-14 was *in vitro* transcribed as in Ref. 36. Radioactive RNA preparations were generated by *in vitro* transcription in the presence of α-[^{32}P]ATP (specific activity, 3000 Ci/mmol). All of the transcripts were gel electrophoretically purified, eluted from the gel slices, and EtOH-precipitated. RNA folding was performed in EB by heating to 75 °C (5min) and cooling to room temperature at 1 °C/min.

Substrate RNA Competition of in Vitro RNA Editing—Precleaved RNA editing *in vitro* insertion and deletion assays were conducted as described (7, 30) using preannealed, synthetic pre-mRNA/gRNA hybrid RNAs. The reactions were initiated by a 5 min preincubation at 27 °C with 20 S editosomes in EB in the presence of 0.5 mM ATP and 40 μM UTP. Competitor pre-mRNA/gRNA hybrid RNA was added (up to a 380-fold molar excess) and incubated for an additional 2 h at 27 °C. The reactions were terminated by phenol extraction, EtOH-precipitated, and analyzed in denaturing (8 M urea), 15% (w/v) polyacrylamide gels followed by phosphorimaging.

RNA Unfolding—^{32}P-Labeled pre-mRNA (2 nM) was incubated with 0–40 nM 20 S editosomes at 27 °C for 0–60 min followed by structure-specific enzymatic probing at limiting enzyme concentrations. RNA cleavage was performed with 60 units/ml RNase T1 (Fermentas) or 3 units/ml cobra venom RNase V1 (Ambion) for 2 min at room temperature. The samples were analyzed in urea-containing (8 M), 6% (w/v) polyacrylamide gels followed by phosphorimaging.

Surface Plasmon Resonance— gRNAs, pre-edited, and edited mRNAs were 3′-oxidized at 4 °C overnight in the dark in 10 mM $NaIO_4$, 50 mM NaOAc, pH 4.8, 10 mM $MgCl_2$, 100 mM NaCl (37). The samples were desalted by size exclusion chromatography and EtOH-precipitated. RNAs were covalently attached to the surface of an amino silane-derivatized microcuvette (Neosensors, UK) in coupling buffer (100 mM $Na_xH_yPO_4$, pH 7.0, 150 mM NaCl, 50 mM $NaBH_3CN$) for 3 h at 27 °C. Binding was monitored in real time as a shift in the resonant angle. The data were fitted by nonlinear regression, and k_{diss} and k_{ass} values were determined by plotting observed on rates ($k_{on(obs)}$) as a

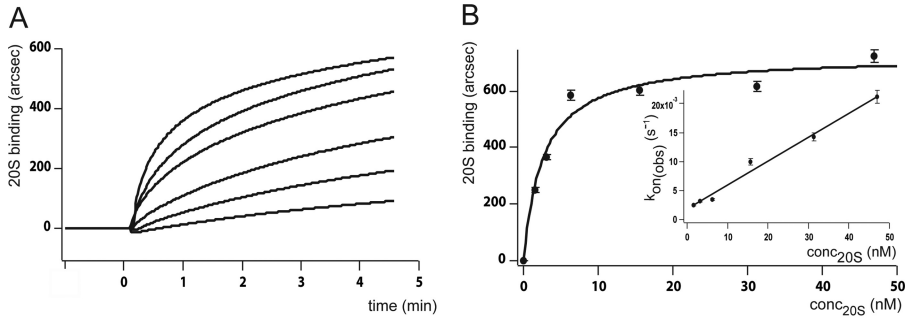

C

RNA	length (nt)	K_d (nM)	k_{ass} ($M^{-1}s^{-1}$)	k_{diss} (s^{-1})	$t_{1/2}$ (min)
COI	1647	8.6	$4.3•10^5$	$3.7•10^{-3}$	3.1
A6-UE	344	5	$4.1•10^5$	$2.1•10^{-3}$	5.5
A6-FE	762	3.6	$7.7•10^5$	$2.8•10^{-3}$	4.1
Cyb-UE	1080	2.9	$4.2•10^5$	$1.2•10^{-3}$	9.6
Cyb-FE	1113	12	$6.0•10^5$	$7.2•10^{-3}$	1.6
A6-UE/gRNA	344/70	5.5	$4.4•10^5$	$2.4•10^{-3}$	4.8
gRNA	70	6.5	$7.6•10^5$	$4.9•10^{-3}$	2.4

FIGURE 1. **Real time surface plasmon resonance monitoring of the binding of 20 S editosomes to mitochondrial RNAs.** *A*, sensograms of the concentration dependent binding of 20 S editosomes to A6-UE mRNA (*top* to *bottom*: 50, 30, 15, 6, 3, and 2 nM editosomes). *B*, corresponding binding curve of the 20 S/A6-UE association. *Inset*, plot of $k_{on(obs)} = f(conc_{20S})$ for the calculation of k_{on} and k_{diss}. The *error bars* represent relative errors as percentages. *C*, summary of the binding characteristics of the 20 S/RNA interaction for different mitochondrial transcripts.

function of the complex concentration ($k_{on(obs)} = k_{ass}$ [RNA/20 S complex] + k_{diss}). Equilibrium dissociation constants (K_d) were calculated as $K_d = k_{diss}/k_{ass}$. The number of binding sites was calculated based on the equation $K_a R_{max} - R_{eq}K_a = R_{eq}/$[20 S]. A plot of R_{eq} *versus* R_{eq}/[20 S] yields a slope of $-K_a$ with a *x* intercept of R_{max} and a *y* intercept of $K_a R_{max}$. RNA/editosome half-lives ($t_{½}$) were determined as $t_{½} = \ln 2/k_{diss}$.

Streptavidin Gold Labeling and Transmission EM—20 S editosome preparations were dialyzed to remove glycerol and incubated with synthetic 5′-biotinylated (bio) substrate RNAs (bio gRNA, bio pre-edited mRNA, or gRNA/bio pre-edited mRNA hybrid molecules) in EB in a 1:1 molar ratio (27 °C, 60 min). Editosome-bio RNA complexes were allowed to adhere to carbon films and were further incubated with streptavidin-derivatized 6-nm gold particles (Aurion, Wageningen, The Netherlands) (room temperature, 30 min). Following an additional 20 min incubation with 2% (w/v) uranyl acetate in H_2O, the streptavidin-decorated editosome-bio RNA complexes were transferred onto 400 mesh square copper grids (Plano, Wetzlar, Germany) and sandwiched with another carbon film. Air-dried specimens were analyzed by transmission electron microscopy at 50 keV, and pictures were taken at 85,000× magnification. The images were processed using ImageJ (38). The images were smoothed to reduce noise and false colored by applying the ImageJ interactive three-dimensional surface plot plug-in.

Atomic Force Microscopy (AFM)—Editosomes were dialyzed in EB to remove glycerol and incubated with substrate RNAs (pre-mRNA, gRNA, and pre-mRNA/gRNA hybrids) in a 1:1 molar stoichiometry (60 min at 27 °C). Editosome-RNA complexes were deposited onto freshly cleaved mica and allowed to adhere for 5 min. The mica was washed (three times with 1 ml of EB) and dried in a mild stream of N_2. The images were taken in tapping mode in air using a MFP-3D AFM (Asylum Research, Santa Barbara, CA) and OMCL-AC240TS silicon cantilevers (Olympus, Hamburg, Germany) with a nominal spring constant of 2 N/m and a resonance frequency of approximately 70 kHz. All of the images were scanned at a frequency of 1 Hz and were analyzed using the MFP-3D software (Asylum Research). Apparent particle volumes (V_{app}) were calculated as $V_{app} = \pi h(w)^2/6$ (where *h* is height, and *w* is width), assuming oblate spheroid shapes of the complexes (39). Contour length measurements were performed by manually tracing using MFP-3D and fitting of the contour length histogram to a Gaussian distribution.

RESULTS

20 S Editosomes Bind Mitochondrial RNAs Indiscriminately—T. brucei 20 S editosomes have been shown to bind short (≤30 nucleotides), synthetic oligoribonucleotides that mimic substrate gRNA and pre-mRNA molecules as well as short, antiparallel gRNA/pre-mRNA hybrid RNAs with nanomolar affinity (27). To analyze the binding of 20 S editosomes to their natural substrates, we examined their interaction with full-length mRNA and gRNA molecules. For that we generated a set of mitochondrial mRNAs that are edited to a different extent. We cloned the UE and FE versions of the ATPase subunit 6 (A6) transcript, which undergoes editing throughout its entire primary sequence (447 U insertions and 28 U deletions) (40). Furthermore, we cloned the UE and FE versions of the Cyb transcript, which contains a single editing domain at its 5′-end (34 U insertions) (41), and lastly we used the COI transcript, which is never edited. To derive quantitative data we performed real time binding experiments using a surface plasmon resonance-based read-out system. Fig. 1*A* shows representative binding isotherms of 20 S editosomes to surface immobilized A6-UE mRNA. The two binding partners interact in a concentration-dependent fashion. Binding is complete within 3–4 min and is characterized by an association rate constant (k_{ass}) of 4.1×10^5 M^{-1} s^{-1} and a macroscopic equilibrium dissociation constant (K_d) of 4.9 nM (Fig. 1*B*). Identical experiments with full-length gRNA gA6-14 and gA6-14 hybridized to A6-UE resulted in K_d values of 6.5 and 5.5 nM. This indicates high affinity binding and

confirms that 20 S editosomes do not discriminate between full-length mRNA, full-length gRNA, and full-length mRNA/gRNA hybrid molecules. Furthermore, we showed that Cyb-UE transcripts and the never edited COI transcript interact with 20 S editosomes with K_d values of 2.9 and 8.6 nM, indicating that pan-edited pre-mRNAs, pre-mRNAs that are edited to a lower extent, and never edited transcripts are bound with similar affinities. Experiments with A6-FE and Cyb-FE resulted in K_d values of 3.6 and 12 nM with calculated half-lives ($t_{1/2}$) for the different complexes varying between 2 and 10 min. Taken together (Fig. 1*C* and supplemental Fig. S1), the determined association rate constants (k_{ass}) vary by a factor of 2, the k_{diss} values vary by a factor of 6, and the corresponding macroscopic K_d values vary by a factor of 4. This indicates that 20 S editosomes by and large interact with different RNA species in a kinetically and thermodynamically nondiscriminative fashion.

The different 20 S/RNA binding isotherms can be further analyzed to determine the number of 20 S binding sites/RNA substrate molecule (supplemental Fig. S2). For gRNA gA6-14 (70 nucleotides), A6-UE (344 nucleotides), and the A6-UE/gRNA hybrid molecule (344/70 nucleotides) we derived ≤1 bound editosome per RNA molecule. For Cyb-FE (1113 nucleotides) and Cyb-UE (1080 nucleotides), we identified two interaction sites and the never edited COI transcript (1647 nucleotides) was bound by four editosomes. This demonstrates that multiple editosomes can bind to a single mRNA and further suggests that the editosome/mRNA interaction is characterized by a defined spatial arrangement of ≤470 nucleotides of RNA per 20 S particle.

20 S Editosomes Have One RNA-binding Site—As a follow up, these data raised the question of the number of RNA-binding site(s) per 20 S editosome. To address this issue, we directly visualized editosome-bound RNA by gold labeling in combination with transmission electron microscopy. Affinity-purified 20 S complexes were incubated with 5′-biotin-derivatized, synthetic oligoribonucleotides mimicking gRNA, pre-mRNA, and gRNA/pre-mRNA hybrid RNAs. After binding we localized the biotin-modified RNAs with the help of streptavidin-derivatized gold cluster with a mean diameter of 6 nm. Fig. 2 (*A* and B) shows representative electronmicrographs of gold-labeled mRNA/gRNA hybrid molecules bound to 20 S editosomes. Fig. 2*C* shows individual gold-labeled editosome-RNA complexes derived from experiments with all three RNA species (gRNA, pre-mRNA, and gRNA/mRNA hybrid RNAs). The complexes are characterized by dimensions of 21 × 26 nm (27), and as expected, the bound gold cluster covers approximately one-fourth of the surface area of the individual particles (Fig. 2*D*). For each RNA binding experiment, we analyzed 10^3 editosome-RNA complexes. Approximately 97% of the complexes showed one bound gold cluster indicating that editosomes have a single substrate RNA-binding site.

This result has the following consequences: First, it implicates that editing substrate RNAs should compete for the editosome-binding site, and second, it suggests that the two types of editing reactions (U deletion and U insertion) might be catalyzed within a single, bifunctional reaction center. To test this hypothesis we conducted substrate RNA competition experiments in combination with *in vitro* RNA editing activity assays

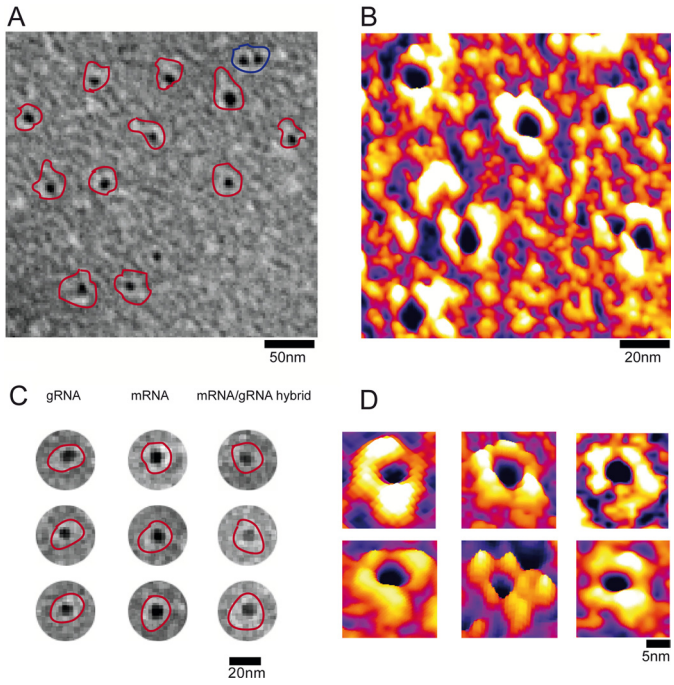

FIGURE 2. *A*, transmission electronmicrograph of 20 S editosomes (*red circles*) with bound gold-derivatized mRNA/gRNA hybrid RNAs. The complexes are characterized by one bound gold cluster (average diameter of 6 nm), which indicates one RNA-binding site. The complex circled in *blue* is an aggregate of two editosomes. *B*, false color image of several gold-derivatized editosome-RNA complexes. *C*, individual gold-labeled editosome-RNA complexes for all three RNA ligands: gRNA, pre-mRNA and gRNA/pre-mRNA hybrid RNA. *D*, false color images of individual gold-labeled editosome-RNA complexes. Please note that *B* and *D* do not represent three-dimensional images.

(7, 30). The experiments are based on the rationale that a pre-bound insertion type RNA editing substrate should be competed out of its binding site by an excess of deletion type RNA substrate (and vice versa). Supplemental Fig. S3 shows the result. As anticipated, both the U deletion editing activity as well as the U insertion activity can be inhibited by increasing amounts of the "reciprocal" editing substrate. In both cases half-maximal inhibition was achieved at a ≤10-fold molar excess of competitor RNA, which verifies that the different substrate RNAs act as archetypical competitive inhibitors. Furthermore it shows that the identified substrate-binding site is at or in close proximity to the catalytically active reaction center of the editosome.

Atomic Force Microscopy of Native Editosomes—To derive a more detailed picture of the RNA/editosome interaction, we aimed at visualizing individual RNA/editosome complexes by AFM. As a first experiment we analyzed affinity-purified (TAP-tagged) editosome preparations in the absence of exogenously added RNA. Fig. 3*A* shows a representative result. As anticipated from the published EM data (27) TAP-tagged editosome preparations contain both 20 and 35–40 S complexes. Both particles are characterized by a well defined, roundish appearance and can be distinguished by their diameter and height (Fig. 3, *B* and *C*). 20 S complexes have a mean diameter of 24.4 nm and an average height of 4 nm (Fig. 3*D*). 35–40 S particles have a mean diameter of 49.3 nm and an average height of 7 nm (Fig. 3*E*). These numbers deviate from the published EM-based measurements (27) and are likely influenced by two phenomena: (i) flattening of the complexes during the AFM analysis (39,

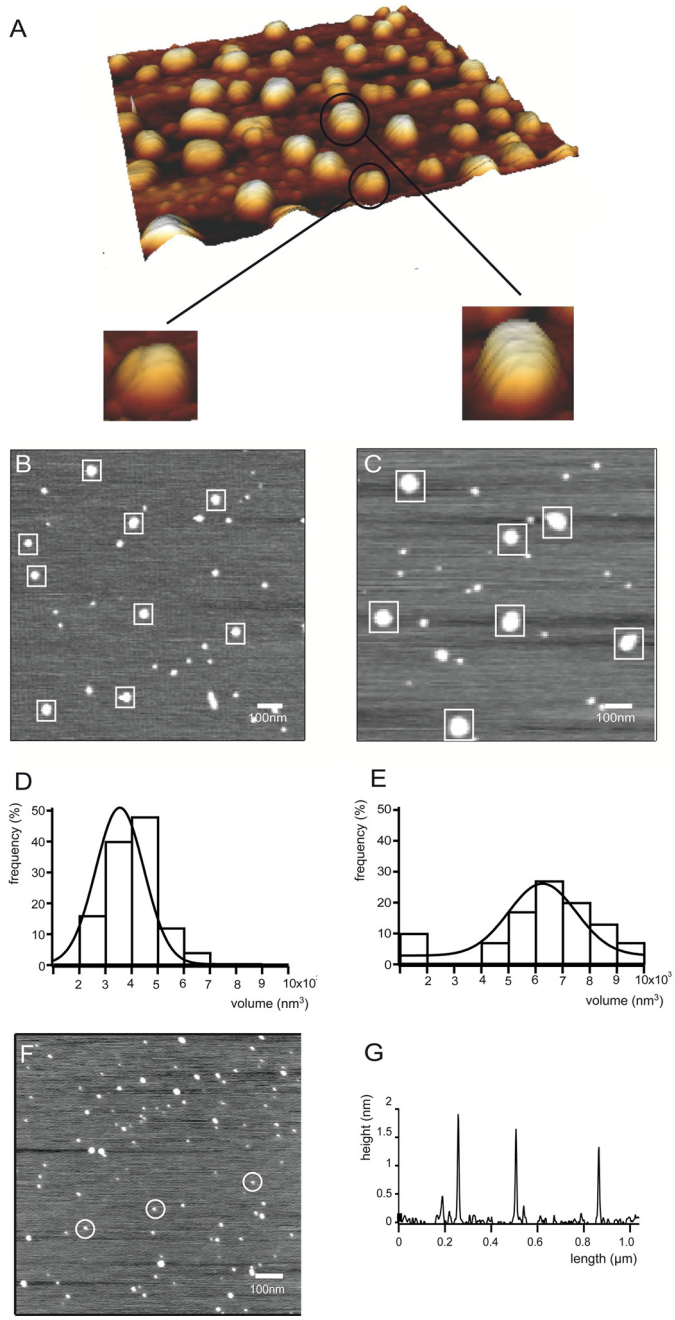

FIGURE 3. **AFM of native editosomes and substrate RNAs.** *A*, three-dimensional AFM image of an affinity-purified (TAP-tagged) editosome preparation deposited on a mica surface. The isolate contains both 20 and 35–40 S editosomes. Two individual complexes of each kind are encircled and outcropped (*left panel*, 20 S editosome; *right panel*, 35–40 S editosome). *B* and *D*, AFM image (height view) of purified 20 S editosomes. Individual complexes (*white squares*) have a mean diameter of 24.4 nm (*B*) and an average volume of 3–4 × 10^3 nm^3 (*D*). *C* and *E*, AFM image (height view) of purified 35–40 S editosomes. The particles have a mean diameter of 49.3 nm (*D*) and a mean volume of 6–7 × 10^3 nm^3 (*E*). *F*, AFM image (height view) of A6-UE mRNA on mica. The RNAs appear as round structures with an average diameter of 13 nm and an average height of ≤2 nm. *G*, height trace of the three encircled A6-UE mRNA molecules in *F*.

42, 43) and (ii) shrinking of the particles caused by dehydration on the mica surface (44, 45). Nevertheless, the dimensions can be used to calculate apparent volumes (V_{app}) for the complexes, which revealed Gaussian distributions with an average volume of 3–4 × 10^3 nm^3 for the 20 S editosome and 6–7 × 10^3 nm^3 for the 35–40 S editosome (Fig. 3, *D* and *E*). In agreement with recently published data (46), AFM of pure RNA preparations showed that the molecules are highly folded. Fig. 3*F* illustrates as an example a preparation of the A6-UE transcript. The molecules appear as a monodisperse population of small roundish structures with diameters varying between 7 and 20 nm (mean diameter, 13 nm) and an average height of ≤2 nm (Fig. 3*G*).

Atomic Force Microscopy of Editosome-RNA Complexes—For the visualization of individual editosome-RNA complexes, we incubated the two reactants at equimolar concentrations for 0–60 min. Fig. 4 shows representative experiments using the transcripts A6-UE, A6-FE, Cyb-UE, and COI. At zero incubation time, the two reactants are well separated and can be distinguished by their characteristic dimensions (Fig. 4*A*). After 5 min (Fig. 4*B*) binding can be detected, which surprisingly is accompanied by an unfolding of the RNA structure (see *inset* in Fig. 4*B*). The highly folded RNAs (Fig. 3*F*) are opened up through the interaction with 20 S editosomes, and the reaction increases over time (Fig. 4*C*). Furthermore, and in line with the binding data, more than one editosome interacts with a fully unfolded mRNA molecule. Fig. 4 (*D* and *F*) shows a representative example of an A6-UE mRNA-editosome complex after 5 min of incubation. Multiple 20 S particles (on average 2–3) are bound to one A6-UE transcript and are distributed over the entire length of the RNA. No preferential binding sites were identified, confirming the non-sequence-specific binding of RNA by 20 S editosomes. After 60 min, RNA-associated structures with dimensions even greater than that of a 20 S editosome were observed (Fig. 4, *E* and *G*). These structures likely represent editosome multimers (likely dimers and trimers). All tested mRNAs (Fig. 4, *H*, *J*, and *K*) were substrates of the unwinding reaction although with different kinetic (after 60 min): Cyb-UE > A6-UE > COI = A6-FE. This likely reflects the different higher order foldings, *i.e.*, thermodynamic stabilities of the various RNAs. Measuring the contour length of three of the transcripts (COI, A6-UE, and Cyb-UE) after 60 min identified that the A6-UE and Cyb-UE transcripts were fully unfolded, whereas the COI mRNA was resolved to only approximately 30% of its theoretical length (supplemental Fig. S4). The average thickness of an unfolded RNA strand was determined as ≤2 nm in line with previously published data (47).

20 S Editosomes Execute RNA Unwinding Activity—To confirm the editosome-driven RNA unfolding reaction, we measured RNA unfolding by biochemical means. The assay is based on the rationale that opening up the higher order structure of an RNA should make the molecule RNase susceptible. For that, we generated radioactively labeled mRNA preparations, which were incubated with 20 S editosomes in the presence of structure-specific RNases. The reaction was performed at limiting enzyme conditions to ensure that in the absence of editosomes, all input RNA remained undigested during the incubation. Fig. 5 shows a representative experiment using the A6-UE transcript as an example. The RNA was hydrolyzed with RNase T1 (Fig. 5*A*), which degrades RNA 3′ of single-stranded G-residues, as well as with cobra venom RNase V1 (Fig. 5*D*), which cleaves base-paired nucleotides. The generated cleavage products were separated in denaturing polyacrylamide gels, and the percentage of degradation was determined. Incubation of 2 nM

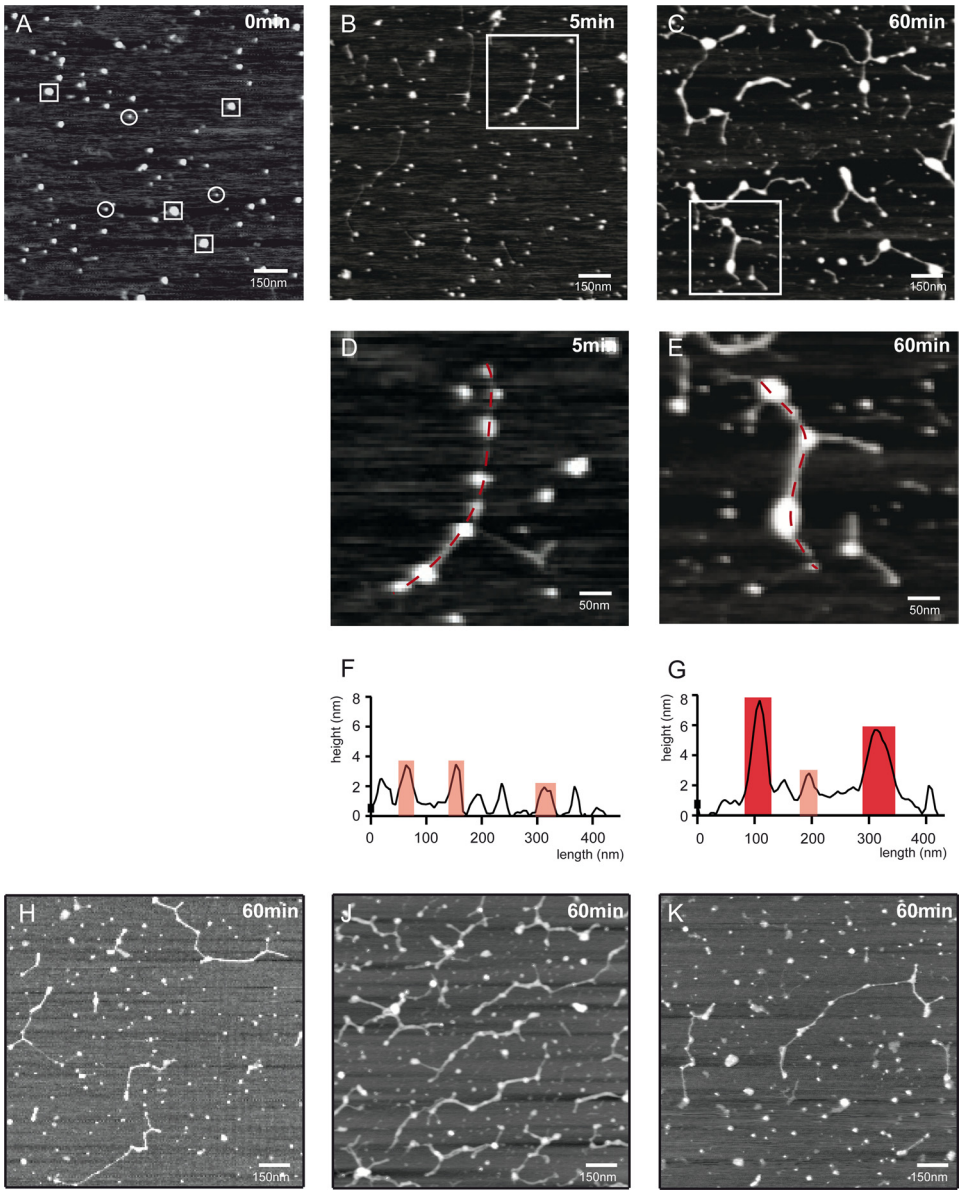

FIGURE 4. **AFM of editosome-RNA complexes.** *A–C*, AFM images of 20 S editosomes (*small squares*) incubated with A6-UE mRNA (*circles*) for 0, 5, and 60 min. *D*, enlargement of the highlighted (*large square*) editosome-A6-UE mRNA complex in *B*. The image shows a single A6-UE mRNA molecule bound by multiple editosomes. *E*, enlargement of the highlighted (*large square*) editosome-A6-UE mRNA complex in *C*. The image shows the formation of editosome multimers/aggregates on a single A6-UE mRNA after 60 min of incubation. *F* and *G*, contour length measurements (stippled lines) of the complexes shown in *D* and *E*. *Red*, 20 S editosomes; *dark red*, editosome multimers; *no highlighting*, higher order RNA structure elements. *H*, *J*, and *K*, AFM images of editosome-RNA complexes for different pre-mRNAs after 60 min of incubation: COI (*H*), Cyb-UE (*J*), and A6-FE (*K*).

A6-UE mRNA with increasing concentrations (0 – 40 nM) of 20 S editosomes for 60 min at 27 °C led to an increased degradation of the RNA by the two ribonucleases (Fig. 5, *B* and *E*). The degradation follows a general decay function (Fig. 5, *C* and *F*), and the RNase T1 digestion is ≥90% complete at an editosome concentration of ≥10 nM. The RNase V1 digest requires 40 nM editing complex to achieve the same result. Half-maximal degradation is accomplished at approximately 5 nM editosomes in both experiments (Fig. 5, *C* and *F*). The *insets* in Fig. 5 (*C* and *F*) show the results of two time course experiments. The degradation follows a decay kinetic with half-maximal degradation after approximately 15 min and approximately 80 –90% degradation after 60 min in both cases. As expected for a RNA chaperone-type activity (48), the reaction does not require exogenous ATP.

DISCUSSION

20 S editosomes are the catalytic machinery of the RNA editing reaction. They represent high molecular mass, "protein only" assemblies that contain all key activities to convert pre-edited transcripts into edited mRNAs. A crucial step in the reaction cascade is the binding of pre-edited mRNAs and gRNAs to form "substrate RNA-loaded" editosomes. Here we analyzed the thermodynamic and kinetic characteristics, as well as the molecularity of the editosome/RNA interaction in detail. 20 S editosomes have previously been shown to bind short, synthetic gRNA, pre-mRNA, and gRNA/pre-mRNA hybrid oligonucleotides with nanomolar affinity (K_d) (27). In the present study we used a panel of "*in vivo* sized" substrate

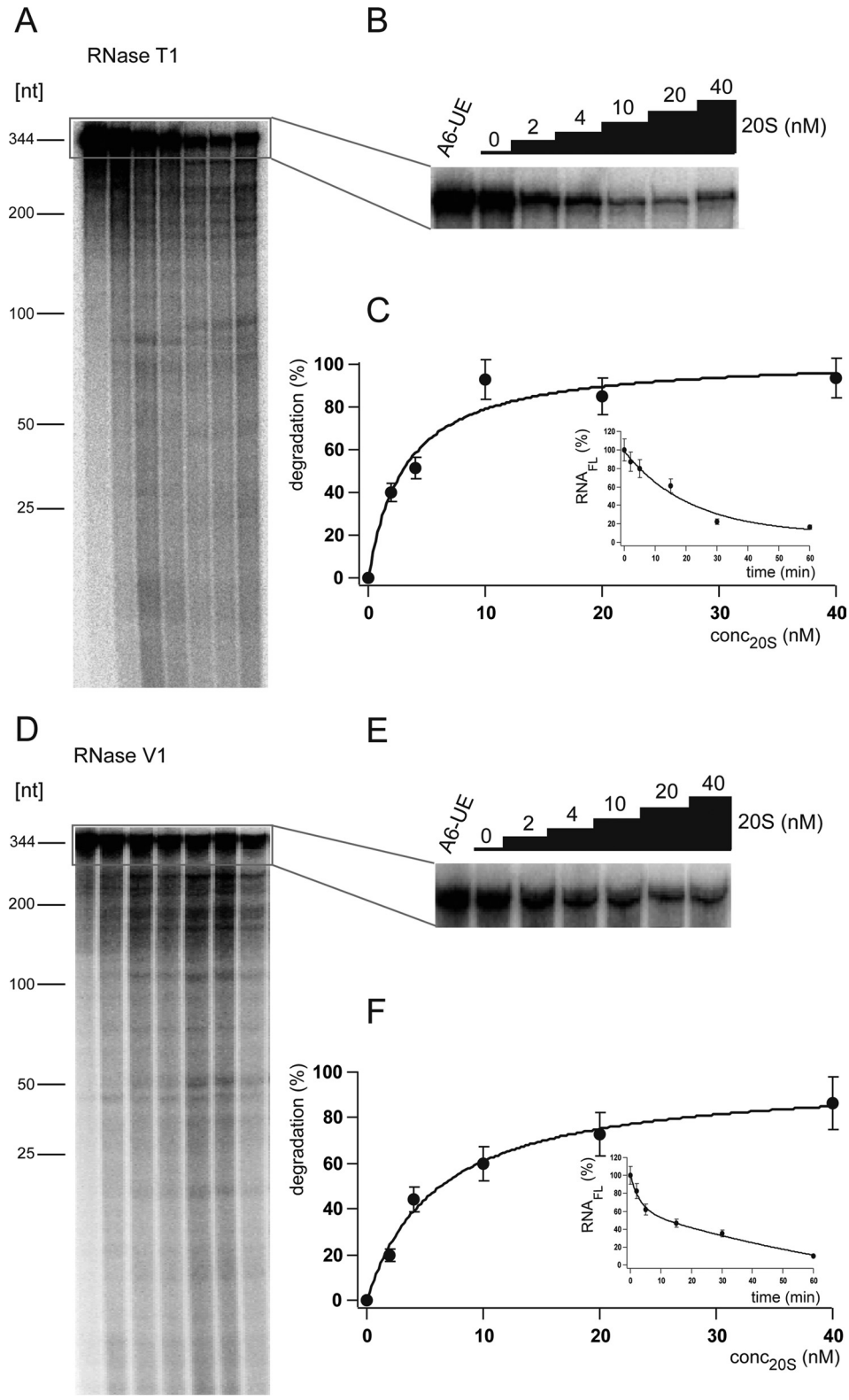

FIGURE 5. **Editosome-driven RNA unwinding.** Autoradiograms of ^{32}P-labeled A6-UE mRNA after incubation with increasing concentrations of 20 S editosomes (0–40 nM) are shown. RNA unwinding was monitored by structure-specific RNase digestion using RNase T1 (*A*) and RNase V1 (*D*). Nonsaturated exposures of the full-length mRNA (344 nucleotides) are shown in *B* and *E*. Shown is a plot of the percentage of degradation as a function of the 20 S editosome concentration. *C*, RNase T1 digestion. *F*, RNase V1 digestion). *Insets*, kinetic of the editosome-dependent RNA unwinding reaction. *FL*, full-length. The *error bars* show the relative errors as percentages.

RNAs (70–1647 nucleotides). We determined that full-length mRNAs, gRNAs, and mRNA/gRNA hybrid RNAs interact with editosomes with similar (nanomolar) K_d values and almost identical association and dissociation rate constants (k_{ass}/k_{diss}). Furthermore, we showed that editosomes do not discriminate between transcripts that are extensively (A6) or moderately

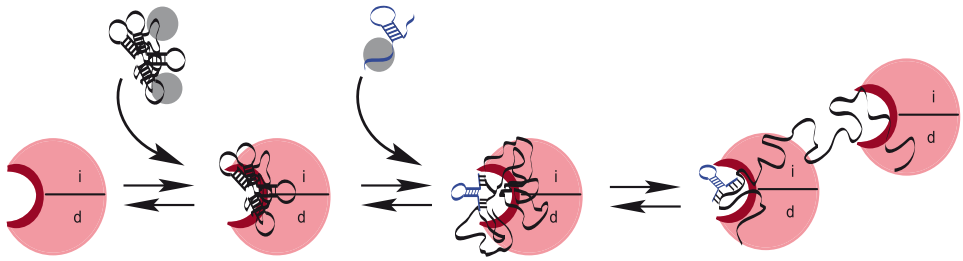

FIGURE 6. **Cartoon of the binding characteristics and downstream events of the editosome/RNA interaction.** 20 S editosomes (*red spheres*) bind substrate RNAs with high affinity. The interacting RNAs (pre-mRNAs, *black*; gRNAs, *blue*) likely bind in the form of ribonucleoprotein complexes (*gray spheres*), and the interaction takes place at a single RNA-binding site (*dark red*). Upon binding, an editosome-intrinsic RNA unwinding activity catalyzes the unwinding of the bound RNAs, which ultimately enables multiple editosomes to bind to one pre-mRNA. *i*, insertion; *d*, deletion subdomain of the 20 S editosome.

edited (Cyb) or between pre-edited and edited versions of the same transcript. Even never edited mRNAs (COI) bind with nanomolar affinity. Despite the high affinity of the different 20 S-RNA complexes, the lack of substrate specificity demonstrates that editosomes can interact with RNA molecules in a nonselective fashion, and it further shows that RNA binding is not restricted to exclusively RNA editing substrate RNAs. This suggests an additional, perhaps in parts even RNA editing-independent function of the editosome (see below). Whether that reflects the situation *in vivo* remains to be tested. Given the fact that the RNA editing machinery has been shown to interact with various gRNA- and mRNA-containing ribonucleoprotein complexes, it seems plausible that some level of discrimination can be achieved by binding protein-associated RNAs rather than "naked" RNA molecules. Potential candidates are the identified mitochondrial RNA binding and mRNA-stabilizing proteins and complexes as well as chaperone-type RNA annealing factors and RNA helicases (reviewed in Refs. 2 and 49–51).

We also found no evidence for a discrimination between transcripts that undergo insertion type editing only and transcripts that undergo both insertion and deletion type RNA editing. This raised the questions of whether editosomes have one or multiple reaction centers and whether the two different editing reactions are catalyzed by the same or by separate (sub)complexes with separate RNA-binding sites. Using transmission electron microscopy, we were able to demonstrate that editosomes have only one substrate RNA-binding site. All three RNA classes: mRNAs, gRNAs, and mRNA/gRNA hybrids, bind to a single binding domain on the surface of the complex. In only 3% of the examined particles, we identified ≥2 RNA-binding sites. However, these cases could be characterized as aggregates of two or more 20 S complexes. The transmission electron microscopy-derived binding site data were supported by visualizing editosome-RNA complexes by atomic force microscopy. AFM confirmed the presence of a single RNA-binding site on the surface of 20 S editosomes; however, the data also showed that multiple 20 S particles can interact with one RNA transcript. On average two or three 20 S particles bound to one mRNA molecule. No preferential binding domains were identified, and the result was confirmed by surface plasmon resonance-based real time binding experiments. For long substrate RNAs (A6-FE, Cyb-FE, Cyb-UE, and COI), we identified multiple bound editosomes and calculated an approximate mean spacing in the range of 300–500 nucleotides-20 S complex. Importantly, the identified RNA-binding domain is the interaction site for both types of RNA editing substrates. U deletion as well as U insertion pre-mRNA/gRNA model substrates interact with the very same 20 S binding site and as a consequence can act as competitive inhibitors in a reciprocal fashion. Because that also leads to an inhibition of the *in vitro* editing activity this further demonstrates that the identified substrate-binding domain is structurally linked or located near the catalytically active center of the editosome. It also shows that the two types of editing reactions are catalyzed within a single bifunctional reaction center. These data find additional support in the fact that individual gRNAs can guide both deletion and insertion editing within one editing domain (52). After 60 min of incubation we also observed the formation of editosome dimers, trimers, and even assemblies/aggregates of higher complexity. The significance of these "multimeric" complexes awaits further testing.

Lastly, the AFM experiments revealed a so far unknown biochemical activity of the editing machinery: RNA binding is followed by RNA unwinding, which resolves the higher order structure of editosome bound RNAs. This implies that 20 S editosomes execute a chaperone-type RNA unwinding activity. Biochemical unfolding experiments confirmed the presence of the activity and demonstrated that the reaction features defined stoichiometric and kinetic characteristics. RNA contour length measurement further demonstrated that some of the bound transcripts (A6-UE, 344 nucleotides; Cyb-UE, 1080 nucleotides) were fully unfolded (after 60 min), whereas others (COI, 1647 nucleotides) were only partially resolved (approximately 30%). This likely reflects a dependence on the length and/or thermodynamic stability of the bound RNAs. RNA chaperones are proteins that recognize substrate RNA with a broad specificity. They play a role in a multitude of biological processes (for a review see Refs. 48 and 53) and modulate RNA folding to generate biochemically active RNA conformations. Generally, the binding of a chaperone protein destabilizes "incorrectly" folded RNA elements, and therefore, within the context of the editing reaction, the most likely function of the activity is to resolve the highly structured conformations of editosome-bound pre-edited transcripts. Misfolded and/or conformationally trapped RNAs have been shown to be rate-limiting in other RNA-guided biochemical processes (54–56), and as a consequence, it seems plausible that the editing machinery exhibits a catalytic activity to side step this potential roadblock. Whether the activity contributes to other editing-specific reaction steps such as the presentation of anchor sequences or the unfolding of gRNA secondary structure elements (57, 58) cannot be

deduced from the data here. However, based on the observation that never edited mRNAs are substrates of the unwinding reaction, it seems conceivable that the activity represents a rather promiscuous feature of the editing machinery. The reaction possibly contributes to other mitochondrial RNA-driven processes and thus provides a rationale for the above described lack of substrate specificity.

Which of the protein component(s) of the editosome mediates the unfolding activity is an open question. Importantly, the activity is intrinsic to the 20 S editosome and thus is different from the various accessory RNA structure modulating activities that have been identified within the context of the editing cycle (reviewed in Ref. 59). Therefore, all so far functionally unassigned editosomal proteins represent potential candidates. However, of special importance are the six oligonucleotide/oligosaccharide binding (OB)-fold proteins of the 20 S complex (29). OB-fold proteins in other RNA-based biochemical systems have been shown to provide RNA chaperone-type activities (reviewed in Refs. 48 and 60), and TbMP24/KREPA4, one of the editosomal OB-fold proteins, has recently been identified to execute RNA annealing activity (22). Within that context the yeast exosome core protein Rrp44 is of special interest (61, 62). Rrp44 has been shown to catalyze RNA unwinding, and the activity was structurally attributed to a multimeric OB-fold domain. Evidence for a heteromultimeric association of five of the editosomal OB-fold proteins has recently been published (63), which makes this hypothetical "OB-fold core" a prime candidate for the unwinding activity of the 20 S editosome.

Taken together, the presented data support the following scenario (Fig. 6): mitochondrial RNA molecules bind with high affinity to a single RNA-binding site of the 20 S editosome. Both types of editing substrate RNAs (insertion/deletion) interact with the same binding site, suggesting a bifunctional reaction center of the editing machinery. RNA binding is followed by RNA unwinding. The activity is intrinsic to 20 S editosomes and unfolds higher order RNA structure elements, thereby resolving structural roadblocks. Ultimately the activity facilitates the interaction of multiple editosomes with one pre-mRNA. The unwinding activity is promiscuous, which suggests that editosomes may contribute their unwinding function to other RNA-driven mitochondrial pathways in trypanosomes.

Acknowledgments—We thank N. Anspach and C. Hammann for help in setting up the AFM measurements. We acknowledge B. Kaiser and W. Jägermann for making the AFM instrument available to us and C. Voigt for help conducting the RNA inhibition experiments. We thank E. Kruse and P. Morais for critically reading the manuscript.

REFERENCES

1. Hajduk, S., and Ochsenreiter, T. (2010) RNA editing in kinetoplastids. *RNA Biol.* **7,** 229–236
2. Aphasizhev, R., and Aphasizheva, I. (2011) Uridine insertion/deletion editing in trypanosomes. A playground for RNA-guided information transfer. *Wiley Interdiscip. Rev. RNA* **2,** 669–685
3. Blum, B., Bakalara, N., and Simpson, L. (1990) A model for RNA editing in kinetoplastid mitochondria. "Guide" RNA molecules transcribed from maxicircle DNA provide the edited information. *Cell* **60,** 189–198
4. Cruz-Reyes, J., and Sollner-Webb, B. (1996) Trypanosome U-deletional RNA editing involves guide RNA-directed endonuclease cleavage, terminal U exonuclease, and RNA ligase activities. *Proc. Natl. Acad. Sci. U.S.A.* **93,** 8901–8906
5. Piller, K. J., Rusché, L. N., Cruz-Reyes, J., and Sollner-Webb, B. (1997) Resolution of the RNA editing gRNA-directed endonuclease from two other endonucleases of *Trypanosoma brucei* mitochondria. *RNA* **3,** 279–290
6. Aphasizhev, R., and Simpson, L. (2001) Isolation and characterization of a U-specific 3′-5′-exonuclease from mitochondria of *Leishmania tarentolae*. *J. Biol. Chem.* **276,** 21280–21284
7. Igo, R. P., Jr., Weston, D. S., Ernst, N. L., Panigrahi, A. K., Salavati, R., and Stuart, K. (2002) Role of uridylate-specific exoribonuclease activity in *Trypanosoma brucei* RNA editing. *Eukaryot. Cell* **1,** 112–118
8. Brecht, M., Niemann, M., Schlüter, E., Müller, U. F., Stuart, K., and Göringer, H. U. (2005) TbMP42, a protein component of the RNA editing complex in African trypanosomes, has endo-exoribonuclease activity. *Mol. Cell* **17,** 621–630
9. Niemann, M., Brecht, M., Schlüter, E., Weitzel, K., Zacharias, M., and Göringer, H. U. (2008) TbMP42 is a structure-sensitive ribonuclease that likely follows a metal ion catalysis mechanism. *Nucleic Acids Res.* **36,** 4465–4473
10. Aphasizhev, R., Aphasizheva, I., and Simpson, L. (2003) A tale of two TUTases. *Proc. Natl. Acad. Sci. U.S.A.* **100,** 10617–10622
11. Ernst, N. L., Panicucci, B., Igo, R. P., Jr., Panigrahi, A. K., Salavati, R., and Stuart, K. (2003) TbMP57 is a 3′ terminal uridylyl transferase (TUTase) of the *Trypanosoma brucei* editosome. *Mol. Cell* **11,** 1525–1536
12. McManus, M. T., Shimamura, M., Grams, J., and Hajduk, S. L. (2001) Identification of candidate mitochondrial RNA editing ligases from *Trypanosoma brucei*. *RNA* **7,** 167–175
13. Rusché, L. N., Huang, C. E., Piller, K. J., Hemann, M., Wirtz, E., and Sollner-Webb, B. (2001) The two RNA ligases of the *Trypanosoma brucei* RNA editing complex. Cloning the essential band IV gene and identifying the band V gene. *Mol. Cell. Biol.* **21,** 979–989
14. Schnaufer, A., Panigrahi, A. K., Panicucci, B., Igo, R. P., Jr., Wirtz, E., Salavati, R., and Stuart, K. (2001) An RNA ligase essential for RNA editing and survival of the bloodstream form of *Trypanosoma brucei*. *Science* **291,** 2159–2162
15. Niemann, M., Kaibel, H., Schlüter, E., Weitzel, K., Brecht, M., and Göringer, H. U. (2009) Kinetoplastid RNA editing involves a 3′ nucleotidyl phosphatase activity. *Nucleic Acids Res.* **37,** 1897–1906
16. Müller, U. F., Lambert, L., and Göringer, H. U. (2001) Annealing of RNA editing substrates facilitated by guide RNA-binding protein gBP21. *EMBO J.* **20,** 1394–1404
17. Blom, D., Burg, J., Breek, C. K., Speijer, D., Muijsers, A. O., and Benne, R. (2001) Cloning and characterization of two guide RNA-binding proteins from mitochondria of *Crithidia fasciculata*. gBP27, a novel protein, and gBP29, the orthologue of *Trypanosoma brucei* gBP21. *Nucleic Acids Res.* **29,** 2950–2962
18. Müller, U. F., and Göringer, H. U. (2002) Mechanism of the gBP21-mediated RNA/RNA annealing reaction. Matchmaking and charge reduction. *Nucleic Acids Res.* **30,** 447–455
19. Aphasizhev, R., Aphasizheva, I., Nelson, R. E., and Simpson, L. (2003) A 100-kD complex of two RNA-binding proteins from mitochondria of *Leishmania tarentolae* catalyzes RNA annealing and interacts with several RNA editing components. *RNA* **9,** 62–76
20. Ammerman, M. L., Fisk, J. C., and Read, L. K. (2008) gRNA/pre-mRNA annealing and RNA chaperone activities of RBP16. *RNA* **14,** 1069–1080
21. Sbicego, S., Alfonzo, J. D., Estévez, A. M., Rubio, M. A., Kang, X., Turck, C. W., Peris, M., and Simpson, L. (2003) RBP38, a novel RNA-binding protein from trypanosomatid mitochondria, modulates RNA stability. *Eukaryot. Cell* **2,** 560–568
22. Kala, S., and Salavati, R. (2010) OB-fold domain of KREPA4 mediates high-affinity interaction with guide RNA and possesses annealing activity. *RNA* **16,** 1951–1967
23. Missel, A., Souza, A. E., Nörskau, G., and Göringer, H. U. (1997) Disruption of a gene encoding a novel mitochondrial DEAD-box protein in *Trypanosoma brucei* affects edited mRNAs. *Mol. Cell. Biol.* **17,** 4895–4903
24. Li, F., Herrera, J., Zhou, S., Maslov, D. A., and Simpson, L. (2011) Trypano-

some REH1 is an RNA helicase involved with the 3′-5′ polarity of multiple gRNA-guided uridine insertion/deletion RNA editing. *Proc. Natl. Acad. Sci. U.S.A.* **108,** 3542–3547
25. Frech, G. C., and Simpson, L. (1996) Uridine insertion into preedited mRNA by a mitochondrial extract from *Leishmania tarentolae*. Stereochemical evidence for the enzyme cascade model. *Mol. Cell. Biol.* **16,** 4584–4589
26. Göringer, H. U., Katari, V. S., and Böhm, C. (2011) The structural landscape of native editosomes in African trypanosomes. *Wiley Interdiscip. Rev. RNA* **2,** 395–407
27. Golas, M. M., Böhm, C., Sander, B., Effenberger, K., Brecht, M., Stark, H., and Göringer, H. U. (2009) Snapshots of the RNA editing machine in trypanosomes captured at different assembly stages *in vivo*. *EMBO J.* **28,** 766–778
28. Li, F., Ge, P., Hui, W. H., Atanasov, I., Rogers, K., Guo, Q., Osato, D., Falick, A. M., Zhou, Z. H., and Simpson, L. (2009) Structure of the core editing complex (L-complex) involved in uridine insertion/deletion RNA editing in trypanosomatid mitochondria. *Proc. Natl. Acad. Sci. U.S.A.* **106,** 12306–12310
29. Stuart, K. D., Schnaufer, A., Ernst, N. L., and Panigrahi, A. K. (2005) Complex management: RNA editing in trypanosomes. *Trends Biochem. Sci* **30,** 97–105
30. Igo, R. P., Jr., Palazzo, S. S., Burgess, M. L., Panigrahi, A. K., and Stuart, K. (2000) Uridylate addition and RNA ligation contribute to the specificity of kinetoplastid insertion RNA editing. *Mol. Cell. Biol.* **20,** 8447–8457
31. Carnes, J., Trotter, J. R., Peltan, A., Fleck, M., and Stuart, K. (2008) RNA editing in *Trypanosoma brucei* requires three different editosomes. *Mol. Cell. Biol.* **28,** 122–130
32. Carnes, J., Soares, C. Z., Wickham, C., and Stuart, K. (2011) Endonuclease associations with three distinct editosomes in *Trypanosoma brucei*. *J. Biol. Chem.* **286,** 19320–19330
33. Cross, G. A. (1975) Identification, purification and properties of clone-specific glycoprotein antigens constituting the surface coat of *Trypanosoma brucei*. *Parasitology* **71,** 393–417
34. Hauser, R., Pypaert, M., Häusler, T., Horn, E. K., and Schneider, A. (1996) *In vitro* import of proteins into mitochondria of *Trypanosoma brucei* and *Leishmania tarentolae*. *J. Cell Sci.* **109,** 517–523
35. Göringer, H. U., Koslowsky, D. J., Morales, T. H., and Stuart, K. (1994) The formation of mitochondrial ribonucleoprotein complexes involving guide RNA molecules in *Trypanosoma brucei*. *Proc. Natl. Acad. Sci. U.S.A.* **91,** 1776–1780
36. Schmid, B., Riley, G. R., Stuart, K., and Göringer, H. U. (1995) The secondary structure of guide RNA molecules from *Trypanosoma brucei*. *Nucleic Acids Res.* **23,** 3093–3102
37. Odom, O. W., Jr., Robbins, D. J., Lynch, J., Dottavio-Martin, D., Kramer, G., and Hardesty, B. (1980) Distances between 3′ ends of ribosomal ribonucleic acids reassembled into *Escherichia coli* ribosomes. *Biochemistry* **19,** 5947–5954
38. Abramoff, M. D., Magelhaes, P. J., and Ram, S. J. (2004) Image processing with ImageJ. *J. Biophotonics Int.* **11,** 36–42
39. Minh, P. N., Devroede, N., Massant, J., Maes, D., and Charlier, D. (2009) Insights into the architecture and stoichiometry of Escherichia coli PepA*DNA complexes involved in transcriptional control and site-specific DNA recombination by atomic force microscopy. *Nucleic Acids Res.* **37,** 1463–1476
40. Bhat, G. J., Koslowsky, D. J., Feagin, J. E., Smiley, B. L., and Stuart, K. (1990) An extensively edited mitochondrial transcript in kinetoplastids encodes a protein homologous to ATPase subunit 6. *Cell* **61,** 885–894
41. Feagin, J. E., Jasmer, D. P., and Stuart, K. (1987) Developmentally regulated addition of nucleotides within apocytochrome *b* transcripts in *Trypanosoma brucei*. *Cell* **49,** 337–345
42. Matsuura, T., Tanaka, H., Matsumoto, T., and Kawai, T. (2006) Atomic force microscopic observation of *Escherichia coli* ribosomes in solution. *Biosci. Biotechnol. Biochem.* **70,** 300–302
43. Mikamo-Satoh, E., Takagi, A., Tanaka, H., Matsumoto, T., Nishihara, T., and Kawai, T. (2009) Profiling of gene-dependent translational progress in cell-free protein synthesis by real-space imaging. *Anal. Biochem.* **394,** 275–280
44. Moreno-Herrero, F., Colchero, J., and Baró, A. M. (2003) DNA height in scanning force microscopy. *Ultramicroscopy* **96,** 167–174
45. Santos, S., Barcons, V., Christenson, H. K., Font, J., and Thomson, N. H. (2011) The intrinsic resolution limit in the atomic force microscope: implications for heights of nano-scale features. *PLoS One* **6,** e23821
46. Kuznetsov, Y. G., Dowell, J. J., Gavira, J. A., Ng, J. D., and McPherson (2010) A Biophysical and atomic force microscopy characterization of the RNA from satellite tobacco mosaic virus. *Nucleic Acids Res.* **38,** 8284–8294
47. Hansma, H. G., Revenko, I., Kim, K., and Laney, D. E. (1996) Atomic force microscopy of long and short double-stranded, single-stranded and triple-stranded nucleic acids. *Nucleic Acids Res.* **24,** 713–720
48. Rajkowitsch, L., Chen, D., Stampfl, S., Semrad, K., Waldsich, C., Mayer, O., Jantsch, M. F., Konrat, R., Bläsi, U., and Schroeder, R. (2007) RNA chaperones, RNA annealers and RNA helicases. *RNA Biol* **4,** 118–130
49. Hernandez, A., Madina, B. R., Ro, K., Wohlschlegel, J. A., Willard, B., Kinter, M. T., and Cruz-Reyes, J. (2010) REH2 RNA helicase in kinetoplastid mitochondria. Ribonucleoprotein complexes and essential motifs for unwinding and guide RNA (gRNA) binding. *J. Biol. Chem.* **285,** 1220–1228
50. Acestor, N., Panigrahi, A. K., Carnes, J., Zíková, A., and Stuart, K. D. (2009) The MRB1 complex functions in kinetoplastid RNA processing. *RNA* **15,** 277–286
51. Pusnik, M., and Schneider, A. (2012) A trypanosomal pentatricopeptide repeat protein stabilizes the mitochondrial mRNAs of cytochrome oxidase subunits 1 and 2. *Eukaryot. Cell* **11,** 79–87
52. Maslov, D. A., and Simpson, L. (1992) The polarity of editing within a multiple gRNA-mediated domain is due to formation of anchors for upstream gRNAs by downstream editing. *Cell* **70,** 459–467
53. Herschlag, D. (1995) RNA chaperones and the RNA folding problem. *J. Biol. Chem.* **270,** 20871–20874
54. Thirumalai, D., Lee, N., Woodson, S. A., and Klimov, D. (2001) Early events in RNA folding. *Annu. Rev. Phys. Chem.* **52,** 751–762
55. Russell, R., and Herschlag, D. (2001) Probing the folding landscape of the *Tetrahymena* ribozyme. Commitment to form the native conformation is late in the folding pathway. *J. Mol. Biol.* **308,** 839–851
56. Russell, R., Zhuang, X., Babcock, H. P., Millett, I. S., Doniach, S., Chu, S., and Herschlag, D. (2002) Exploring the folding landscape of a structured RNA. *Proc. Natl. Acad. Sci. U.S.A.* **99,** 155–160
57. Hermann, T., Schmid, B., Heumann, H., and Göringer, H. U. (1997) A three-dimensional working model for a guide RNA from *Trypanosoma brucei*. *Nucleic Acids Res.* **25,** 2311–2318
58. Reifur, L., and Koslowsky, D. J. (2008) *Trypanosoma brucei* ATPase subunit 6 mRNA bound to gA6-14 forms a conserved three-helical structure. *RNA* **14,** 2195–2211
59. Göringer, H. U., Brecht, M., Böhm, C., and Kruse, E. (2008) RNA editing accessory factors. The example of mHel61p. In *RNA Editing, Nucleic Acids and Molecular Biology* (Göringer, H. U., ed) pp. 165–179, Springer, Heidelberg
60. Kwon, S. H., Lee, I. H., Kim, N. Y., Choi, D. H., Oh, Y. M., and Bae, S. H. (2007) Translation initiation factor eIF1A possesses RNA annealing activity in its oligonucleotide-binding fold. *Biochem. Biophys. Res. Commun.* **361,** 681–686
61. Lorentzen, E., Basquin, J., Tomecki, R., Dziembowski, A., and Conti, E. (2008) Structure of the active subunit of the yeast exosome core, Rrp44. Diverse modes of substrate recruitment in the RNase II nuclease family. *Mol. Cell* **29,** 717–728
62. Bonneau, F., Basquin, J., Ebert, J., Lorentzen, E., and Conti, E. (2009) The yeast exosome functions as a macromolecular cage to channel RNA substrates for degradation. *Cell* **139,** 547–559
63. Park, Y. J., Pardon, E., Wu, M., Steyaert, J., and Hol, W. G. (2012) Crystal structure of a heterodimer of editosome interaction proteins in complex with two copies of a cross-reacting nanobody. *Nucleic Acids Res.* **40,** 1828–1840